PNAS RESEARCH ARTICLE | MICROBIOLOGY

A virus-induced circular RNA maintains latent infection of Kaposi's sarcoma herpesvirus

Takanobu Tagawa[a], Daniel Oh[a], Sarah Dremel[a], Guruswamy Mahesh[a], Vishal N. Koparde[b,c], Gerard Duncan[d], Thorkell Andresson[d], and Joseph M. Ziegelbauer[a,1]

Edited by Thomas Shenk, Princeton University, Princeton, NJ; received August 2, 2022; accepted December 8, 2022

Non-coding RNAs (ncRNAs) play important roles in host-pathogen interactions; oncogenic viruses like Kaposi's sarcoma herpesvirus (KSHV) employ ncRNAs to establish a latent reservoir and persist for the life of the host. We previously reported that KSHV infection alters a novel class of RNA, circular RNAs (circRNAs). CircRNAs are alternative splicing isoforms and regulate gene expression, but their importance in infection is largely unknown. Here, we showed that a human circRNA, hsa_circ_0001400, is induced by various pathogenic viruses, namely KSHV, Epstein-Barr virus, and human cytomegalovirus. The induction of circRNAs including circ_0001400 by KSHV is co-transcriptionally regulated, likely at splicing. Consistently, screening for circ_0001400-interacting proteins identified a splicing factor, PNISR. Functional studies using infected primary endothelial cells revealed that circ_0001400 inhibits KSHV lytic transcription and virus production. Simultaneously, the circRNA promoted cell cycle, inhibited apoptosis, and induced immune genes. RNA-pull down assays identified transcripts interacting with circ_0001400, including *TTI1*, which is a component of the pro-growth mTOR complexes. We thus identified a circRNA that is pro-growth and anti-lytic replication. These results support a model in which KSHV induces circ_0001400 expression to maintain latency. Since circ_0001400 is induced by multiple viruses, this novel viral strategy may be widely employed by other viruses.

KSHV | HHV8 | circular RNAs | herpesvirus

Significance

Circular RNAs (circRNAs) are single-stranded, closed-circular RNAs, which bind to other RNAs or proteins to regulate their functions. The importance of circRNAs during virus infection has been largely elusive. Here, we identified that a circRNA, hsa_circ_0001400, is induced upon infection with various pathogenic viruses including Kaposi sarcoma herpesvirus (KSHV) and controls viral and human gene expression so that infected human cells have less virus production but better cell growth. KSHV has two phases: latent and lytic cycle. circ_0001400 biases cells to the latent cycle during which viruses express only a limited number of genes to survive for the life of the host. Our results revealed a novel virus-host interaction via circRNAs to maintain latency after infection with an oncogenic virus.

Oncogenic DNA viruses like Kaposi's sarcoma herpesvirus (KSHV) and Epstein-Barr virus (EBV) establish lifelong infection in humans. Around 12% of cancers are associated with oncogenic viruses (1), and KSHV and EBV are associated with various cancers including Kaposi's sarcoma, primary effusion lymphoma (PEL), Burkitt's lymphoma, and nasopharyngeal carcinoma (2). Though primary infections are thought to happen in B lymphocytes, cell types of associated cancers can include B cells, T cells, epithelial cells, and endothelial cells. A crucial strategy for gamma-herpesviruses, KSHV and EBV, is to establish latent infection during which most of the viral genes are silenced and therefore less immunogenic. During the lytic phase, in contrast, reactivated virus expresses upward of 80 transcripts, replicates their genome, and produces infectious progeny. Lytic replication is critical for viral spread; this, however, is at the expense of the host cells. For long-term survival of the virus and infected cells as in the case of KSHV or EBV, maintaining latency is the key strategy.

Non-coding RNAs (ncRNAs) are increasingly deemed important to control infection. For example, Hepatitis C virus depends on a human microRNA (miRNA), hsa-miR-122, for viral RNA accumulation (3) and KSHV's long non-coding RNA, polyadenylated nuclear RNA (PAN RNA), is required for virus productions (4). Viruses also exploit miRNAs to maintain latent infection; hsa-miR-155 is induced by EBV and mimicked by KSHV infection to support latent infection (5–7). Circular RNAs (circRNAs) are novel players in the field of virus-host interactions. CircRNAs are alternative splice isoforms produced from back-splicing. They are single-stranded closed-circular RNAs with the ability to interact with other RNA species or proteins to regulate their functions (8). Some of the first reports of circRNAs demonstrated inhibition of miRNA activity by a circRNA (9, 10). The importance of circRNAs is particularly evident in cancers. A number of human circRNAs have been characterized as oncogenic (e.g., circPVT1, CDR1as) or anti-oncogenic (e.g., circsMARCA5 or circSHPRH) (8).

The contributions of human circRNAs during viral infection are largely unknown. We previously found that KSHV de novo infection differentially regulates dozens of human circRNAs and that the virus encodes its own circRNAs (11–14). One of them, hsa_circ_0001400, was induced upon infection with KSHV and, in a renal carcinoma cell line, reduced KSHV gene expression. The importance of human circRNAs in viral infection is still elusive, particularly in clinically relevant settings such as primary endothelial

Preprint servers: The manuscript was deposited to BioRxiv (doi:10.1101/2022.07.18.500467) and made available for use under a CC0 license.

Author contributions: T.T. and J.M.Z. designed research; T.T., D.O., S.D., and T.A. performed research; V.N.K., G.D., and T.A. contributed new reagents/analytic tools; T.T., D.O., S.D., G.M., and V.N.K. analyzed data; and T.T., S.D., and J.M.Z. wrote the paper.

The authors declare no competing interest.

This article is a PNAS Direct Submission.

[1]To whom correspondence may be addressed. Email: ziegelbauerjm@mail.nih.gov.

This article contains supporting information online at https://www.pnas.org/lookup/suppl/doi:10.1073/pnas.2212864120/-/DCSupplemental.

Published February 1, 2023.

cells: Does hsa_circ_0001400 control KSHV infection? Is host cell physiology affected by circRNAs? What is the mechanism of gene regulation by the circRNA? Does the circRNA function, like some viral miRNAs, to maintain latency?

Here, we mainly focused on early time points after de novo infection of endothelial cells to assess whether circ_0001400 affects the establishment of latent infection. Our high-throughput circRNA profiling and cell types showed regulation of a human circRNA, circ_0001400 by different herpesvirus infections. Functions of circ_0001400 were assessed in human primary endothelial cells regarding viral transcription, virus production, host gene regulation, phenotype of infected cells, and immune responses. To identify RNAs and proteins that interact with circ_0001400, we performed circRNA-RNA-pulldown assays as well as proximity labeling-based circRNA–protein pulldown experiments. All in all, our results encompass that circ_0001400 functions to maintain KSHV latent infection.

Results

Infection of Multiple Herpesviruses Induces the Human circRNA, hsa_circ_0001400. A human circRNA, hsa_circ_0001400 (circ_0001400, circRELL1), encoded from the *RELL1* gene locus, increases upon de novo KSHV infection in epithelial cell lines as well as human primary endothelial cells including human umbilical vein endothelial cells (HUVECs) [Tagawa et al. (11)] and lymphatic endothelial cells (LECs) (Fig. 1*A* and *SI Appendix*, Fig. S1*A*) (15). Circ_0001400 was one of the most abundant circRNAs in HUVECs as well (Fig. 1*B*). We found that circ_0001400 is induced upon infection with various human herpesviruses. The circRNA was more abundant in the EBV-positive Burkitt's lymphoma cell line Akata(+) than in an episome-negative clone Akata(−) (Fig. 1*A*). Similar to gamma-herpesviruses, KSHV and EBV, human cytomegalovirus (beta-herpesvirus) infection showed the tendency to increase circ_0001400 levels in the MRC5 fibroblast cell line at day 3 and 5 after infection (Fig. 1*A*) (16). For alpha-herpesvirus, HSV-1 infection of MRC5 was tested (17). Three out of four replicates showed the increase of circ_0001400 12 h after infection (Fig. 1). Thus, increased levels of circ_0001400 were found after infection with multiple pathogenic human herpesviruses.

How viral infection regulates circRNA transcript levels is elusive. The amount of human circRNA may be regulated by altering transcription rates but also by modulating co-transcriptional steps, particularly back-splicing, which is known to be regulated by RBPs (8). To determine how KSHV regulates circRNA production, we re-analyzed our previous datasets to quantitate circRNAs and counterpart linear mRNAs in KSHV-infected endothelial cells (Fig. 1 *B* and *C*) (19). While circ_0001400 is increased by infection, the mRNA from same gene locus, *RELL1,* was not differentially regulated along with other circRNAs like circZKSCAN1, circRARS, and circXPO1(Fig. 1*B*). This lack of the correlation between fold-changes of circRNAs and linear RNAs is, in fact, global with a Pearson correlation coefficient of 0.055 (Fig. 1*C* and

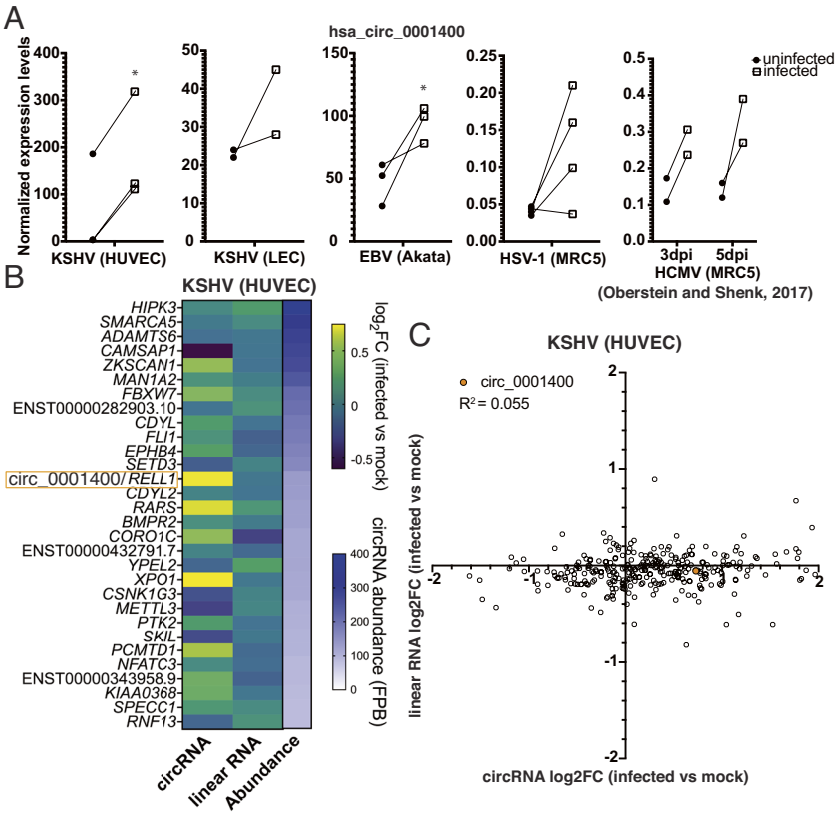

Fig. 1. Herpesviruses induce circ_001400 expression. (*A*) hsa_circ_0001400 transcript levels are shown in KSHV-infected HUVECs at 3 d post-infection (dpi) (microarray), LECs at 3 dpi (RNA-Seq), EBV-positive Burkitt's lymphoma line Akata (microarray), HSV-1-infected fibroblast at 12 h post-infection (RNA-Seq), and HCMV-infected fibroblast at 3 and 5 dpi (RNA-Seq) (16). n = 2 to 4. Significances were computed when n is 2 or more with limma. **P*-value < 0.05. (*B*) Fold-changes of top 30 most abundant human circRNAs in KSHV-infected HUVECs. Transcript levels of circRNAs and corresponding linear messenger RNAs (mRNAs) were quantitated from total RNA-Seq with circExplorer3 (18) as FPBs (fragments per billion mapped base). Fold-changes of circRNAs and linear RNAs (infected vs. mock) are calculated (n = 3), and mean values are shown. Genes are sorted by circRNA FPBs (Abundance), and host genes of both circRNA and linear RNAs are shown on the left. FPBs and ratios are available in Dataset S1. (*C*) Log_2 fold-changes of all detected human circRNAs/counterpart linear mRNAs (KSHV-infected vs. mock HUVECs) are shown as a scatter plot. Data are same as in Fig. 1*B* and Dataset S1. Pearson correlation value was calculated. n = 3 and mean values are shown.

Dataset S1). These results may suggest that KSHV infection changes circRNAs co-/posttranscriptionally (e.g., splicing, localization, or stability).

hsa_circ_0001400 Is Regulated Co-Transcriptionally and Interacts with a Splicing Factor. To test whether circRNAs including circ_0001400 are regulated transcriptionally, co-transcriptionally, or posttranscriptionally, we performed 4SU RNA-Seq. Conventional total RNA-Seq quantitates steady-state level of transcripts, while 4SU-Seq only measures newly transcribed RNAs (Fig. 2*A*). This technique enables us to discern whether KSHV globally alters host circRNA abundance by influencing transcription rates, co-transcriptional (e.g., splicing) or posttranscriptional (e.g., RNA decay) processes. We chose the reactivation model of KSHV-positive iSLK-BAC16 cells since it has similar viral gene expression pattern to infected LEC cells (*SI Appendix*, Fig. S2), but iSLK cells has an advantage that they can be chemically reactivated synchronously unlike a heterogenous de novo infection. The circRNA-to-linear RNA ratio of circ_0001400 increased more in 4SU-labeled (nascent) RNAs than total RNAs (Fig. 2*B*) (20, 21) indicating co-transcriptional increase by KSHV. Most human circRNAs were differentially regulated in a co-transcriptional manner (Fig. 2*B*). This is consistent with the observation in HUVECs where changes of circRNA and linearRNA upon de novo infection did not correlate (Fig. 1 *B* and *C*). During reactivation, 75% of circRNAs were classified to be co-transcriptionally regulated including circ_0001400 (Fig. 2*B*).

The back-splicing step of circRNA maturation is often controlled by RNA-binding proteins (8). To identify proteins interacting with circ_0001400, we utilized a CRISPR-assisted RNA–protein interaction detection method, or CARPID (Fig. 3*A*) (22). CRISPR–Cas13-based targeting of circRNAs is specific and efficient (23). Guide RNAs targeted against circ_0001400 could indeed knock down the circRNA, whereas the counterpart mRNA *RELL1* is minimally affected (*SI Appendix*, Fig. S3*A*). Since CARPID depends on proximity labeling, we can identify proteins that are RBPs directly bound to circ_0001400 as well as indirectly interacting proteins with mass spectrometry. Replicates and different guide RNAs showed high reproducibility, and we identified various proteins including RBPs (*SI Appendix*, Fig. S4). We performed rank-product analysis to select candidate proteins (Fig. 3*B* and Dataset S2) (15) and confirmed the interaction between circ_0001400 and PNN interacting serine and arginine rich protein (PNISR), but not Eukaryotic translation initiation factor 3 subunit K (EIF3K), with RNA-immunoprecipitation (RIP) assays (Fig. 3*C*). Since CARPID captures any proteins that are in proximity of the target, it is possible that EIF3K is indirectly interacting with circ_0001400. Since PNISR is a splicing factor and circRNAs are formed by back-splicing, PNISR may play a role in regulating specific circRNAs such as circ_0001400. Knockdown of PNISR in KSHV-infected endothelial cells showed increase of *RELL1*, but not circ_0001400 (Fig. 3*D* and *SI Appendix*, Fig. S3*B*). PNISR thus showed an ability to skew splicing more to back-splicing (circ_0001400) than forward-splicing (*RELL1*). The 4SU RNA-Seq analysis and identification of a circRNA-interacting splice factor thus suggest that KSHV regulates human circRNAs, including circ_0001400, in a mostly co-transcriptional manner.

KSHV Lytic Gene Expression and Virus Production are Inhibited by circ_0001400. Effects of circ_0001400 early after KSHV infection were assessed using lentiviral transduction and RNAi-mediated knockdown of the circRNA (Fig. 4, *SI Appendix*, Fig. S1 *B–E*, and Dataset S3). The lentivirus vector expresses a cassette that harbors circ_0001400 flanked with ZKSCAN1 introns, which facilitates back-splicing and circularization of RNAs (24). In accordance with our observation with infected SLK cells (11), a renal carcinoma cell line, ectopic expression

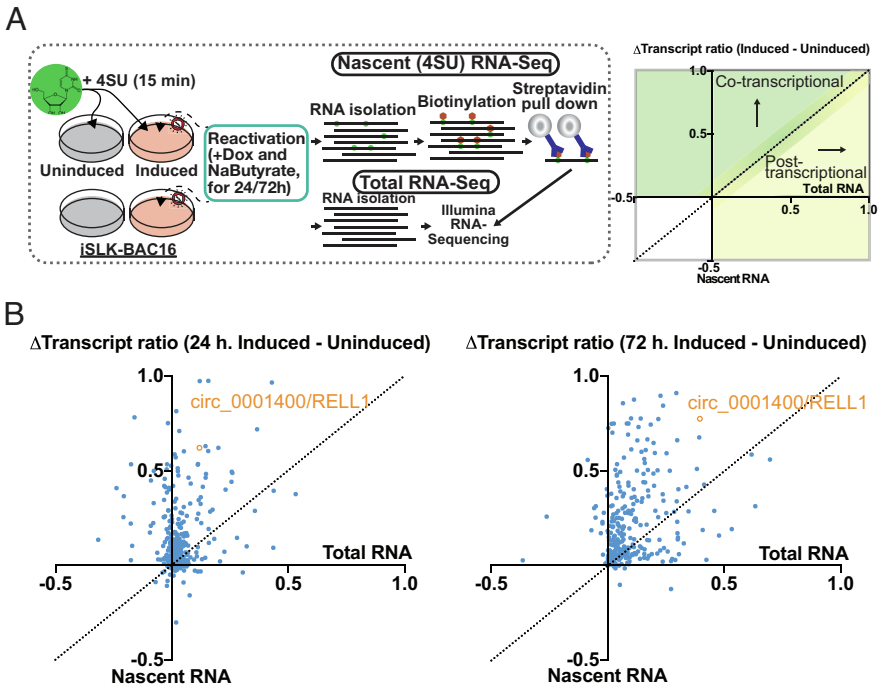

Fig. 2. circ_001400 is co-transcriptionally regulated and interacts with a splicing factor. (*A*) Infographic for sequencing techniques performed (*Left*). *Right* panel shows the quadrant guidance to determine each transcript to be regulated co- or posttranscriptionally. (*B*) Total and 4SU RNA-Seq delta transcript ratio (circular reads/linear reads) for unique human circRNA (1 or 3 d). Positive Δtranscript ratios (induced–uninduced) indicate a shift after lytic reactivation in transcript abundance, favoring the circular transcript. circ_001400 is highlighted in orange. n = 2 and mean values are shown.

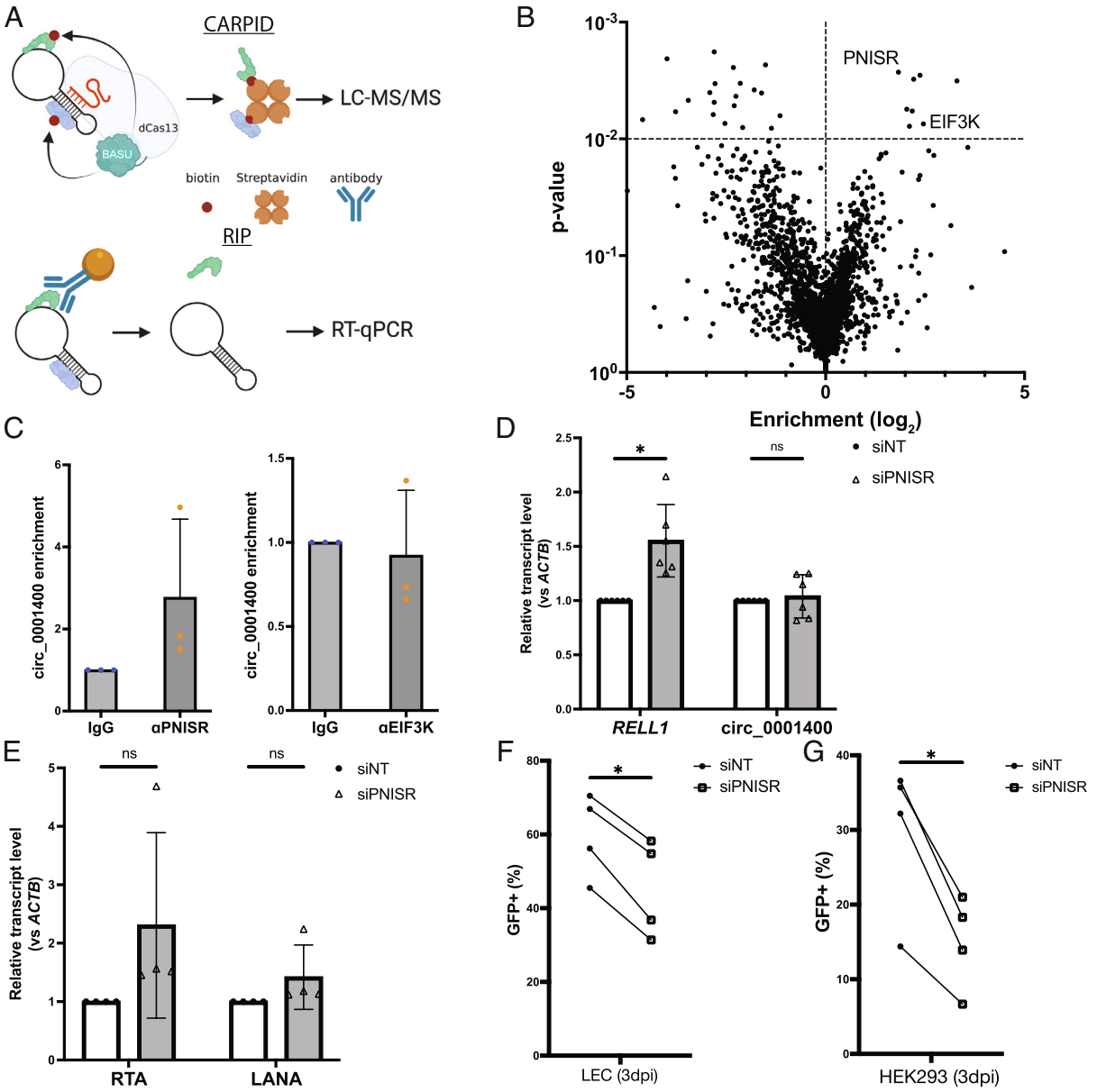

Fig. 3. Protein interactome of circ_0001400. (*A*) Diagram of CARPID and RIP method. CARPID utilizes dead Cas13 conjugated with BASU biotin transferase to biotinylate proteins that are in the proximity of circ_001400 to enrich and determine their identities by liquid chromatography/tandem mass spectrometry. Identified proteins are listed in Dataset S2. Candidate proteins are immunoprecipitated by specific antibodies (RIP), and circ_001400 is confirmed to be co-precipitated by RT-qPCR. (*B*) A volcano plot of proteins that were identified by mass spectrometry (n = 3). Enrichment and significances were calculated by RankProd package. Pre-gRNA (empty) vector and gCirc1400_nc (sequence-randomized) vector were used as negative controls. (*C*) RIP results of candidate proteins. circ_0001400 was ectopically expressed in 293T cells for 24 h, and RIPs were performed against PNISR and EIF3K. circ_001400 transcript levels after RIP are normalized to the isotype IgG antibody condition. n = 3 and significances were calculated with paired-*t* tests. **P*-value < 0.05. (*D* and *E*) *PNISR* knockdown and quantitation of RELL1 transcripts and viral transcripts. LECs were transfected with siRNAs targeting PNISR followed by KSHV infection at MOI of 1.0 i.u for 3 d. Linear and circular transcripts from RELL1 gene locus (RELL1 and circ_000400) (*D*) and viral transcripts (*E*) were quantified. N = 4 to 5. (*F*) Infection rates of PNISR-depleted LEC cells. LECs from (*D* and *E*) were quantified for the green fluorescent protein (GFP) by flow cytometry. N = 4. (*G*) Virion production of PNISR-depleted LEC cells. Conditioned media was collected from LECs from (*F*), and HEK-293 cells were incubated with the conditioned media for 3 d. Infected HEK-293 cells were counted by GFP signals with flow cytometry. N = 4 and significances were calculated with paired-*t* tests. **P*-value < 0.05.

of circ_0001400 (*SI Appendix*, Fig. S1*B*) reduced KSHV gene expression in HUVECs (Fig. 4 *A* and *B*). Viral transcriptome analysis after ectopic expression of circ_0001400 in HUVECs showed suppression of gene expression for most of the KSHV genes (Fig. 4*A*) (15). Consistently, knockdown of circ_0001400 with a circRNA-specific siRNA (*SI Appendix*, Fig. S1*B*) resulted in an increase of viral transcripts (*SI Appendix*, Fig. S1*D* and Dataset S3). The siRNA specifically targets circ_0001400 back-splice junctions, which is unique to circRNAs. The siRNA was proven to be specific to the circRNA and does not affect its counterpart mRNA (11). We observed a difference between lytic and latent genes in suppression: While lytic genes are suppressed by $\log_2$FC of −1.01 ± 0.25, latent genes (K1, K2, K12, K13, latency-associated nuclear antigen (LANA), and ORF72) (25) were reduced only by $\log_2$FC of −0.20 ± 0.14 (*SI Appendix*, Fig. S1*D* and Dataset S3). Importantly, manipulation of circ_0001400 expression levels did not affect infectivity (Fig. 4*C*), suggesting viral gene expression is regulated at a post-entry step.

Though HUVECs are largely considered a latent infection model, KSHV de novo infection is heterogenous, and lytic genes are expressed in a minority of cells (*SI Appendix*, Fig. S2). Since lytic genes are more sensitive to circ_0001400, we

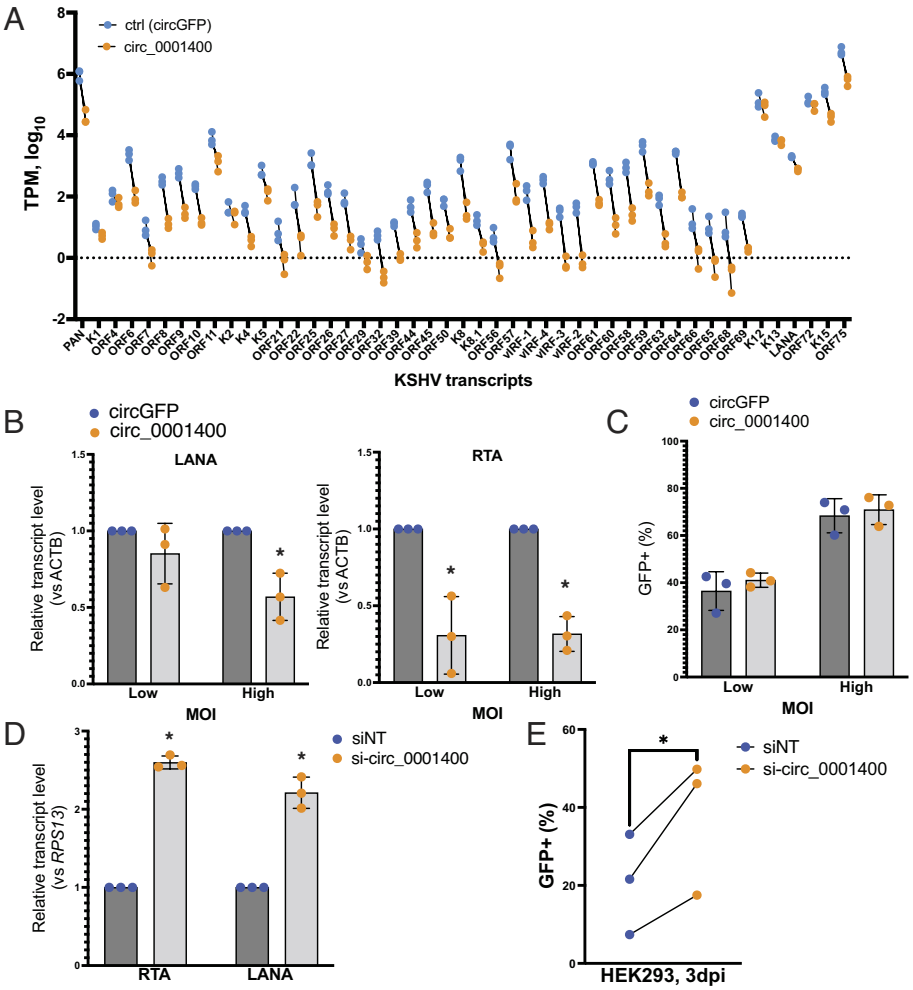

Fig. 4. circ_001400 inhibits viral gene expression and virion production. (*A*) Viral transcriptome analysis after circ_0001400 ectopic expression in KSHV-infected HUVECs (3 d post-infection). n = 3. Transcripts Per Kilobase Million were calculated and only KSHV genes with significant read counts are shown. (*B*) Viral transcript levels after circ_0001400 ectopic expression in KSHV-infected HUVECs. MOI of 0.5 (low) and 1.0 (high) i.u. are used, and RNAs were collected 3 d post-infection (n = 3). (*C*) Populations of GFP-positive, KSHV infected among lentivirus-infected HUVECs are shown. Cells were co-infected with KSHV and lentivirus (circGFP control or circ_0001400) for 3 d (n = 3). GFP signal from circGFP is significantly lower than KSHV BAC16-originated GFP and does not affect the analysis. (*D*) Viral transcript levels after circ_0001400 ectopic expression in KSHV-infected LECs. MOI of 1 i.u. was used for infection, and total RNAs were collected 3 d post-infection (n = 3). (*E*) Virus production from circ_0001400-depleted KSHV-infected LECs. Conditioned media of KSHV-infected LECs (*D*) was collected and used for infection of HEK-293 cells. KSHV-positive, GFP-positive population among HEK-293 cells were measured 3 d post-infection (n = 3). Significances were calculated with paired-*t* tests. **P*-value < 0.05.

hypothesized that those lytic cells are affected by circ_0001400. To assess the effect on the lytic gene expression and virion productions, we used LECs, which spontaneously enter lytic phase after de novo infection more than HUVECs (*SI Appendix*, Fig. S2 *A* and *B*) (26). Expression of circ_0001400 was depleted by siRNAs (*SI Appendix*, Fig. S1*C*), and conditioned media was collected 3 d post-infection. To quantitate functional virions secreted from infected LECs, the conditioned media was used to infect to HEK-293 cells, and KSHV-infected populations were measured using the GFP reporter expressed by the virus. Depletion of the circRNA leads to a significant increase in viral gene expression in LECs as in HUVEC infections (Fig. 4*D* and *SI Appendix*, Fig. S1*B*) as well as newly produced virions (Fig. 4*E*). Taken together, although circ_0001400 slightly down-regulates latent genes, these results indicate that circ_0001400 mainly suppresses lytic infection in primary endothelial cells.

Circ_0001400 Promotes Cell Cycle, Inhibits Apoptosis, and Induces Genes Involved in Immunity. Human circRNAs can regulate expression of multiple genes to control cell physiology (8). To assess host genes affected by circ_0001400, we performed transcriptome analysis of circRNA-manipulated HUVECs (Fig. 5) (15). We observed that 184 genes were consistently and differentially expressed genes (DEGs) by gain- and loss-of-function manipulations of circ_0001400 (Fig. 5*A* and Dataset S4). DEGs include genes involved in cell growth, immune responses, and crucial miRNA components, *AGO1* and *AGO2*, suggesting that circ_0001400 may behave as a regulator of the miRNA machinery (Fig. 5*A*). Gene enrichment analysis suggested pro-cell growth tendency of circ_0001400 with upregulation of phosphoinositide-3-kinase–protein kinase (PI3K)/Ak strain transforming (AKT) signaling and downregulation of PTEN signaling and GADD45 signaling (Fig. 5*B*). Expression of genes that are mediating PI3K/AKT signaling (*MAP2K1*, *NFKB2*, *RELB*) and downstream (*CXCL8*) was up-regulated, whereas inhibitors (*INPP5K* and *TSC2*) (27) are down-regulated by circ_0001400, accordingly (*SI Appendix*, Fig. S5). Since these regulations suggest changes in cell cycle and apoptosis, we evaluated these phenotypes. We found circ_0001400-depletion indeed caused G2 cell cycle arrest and reduced cell counts during starvation in endothelial cells (Fig. 5 *C* and *D*). Apoptosis and cell death were also increased

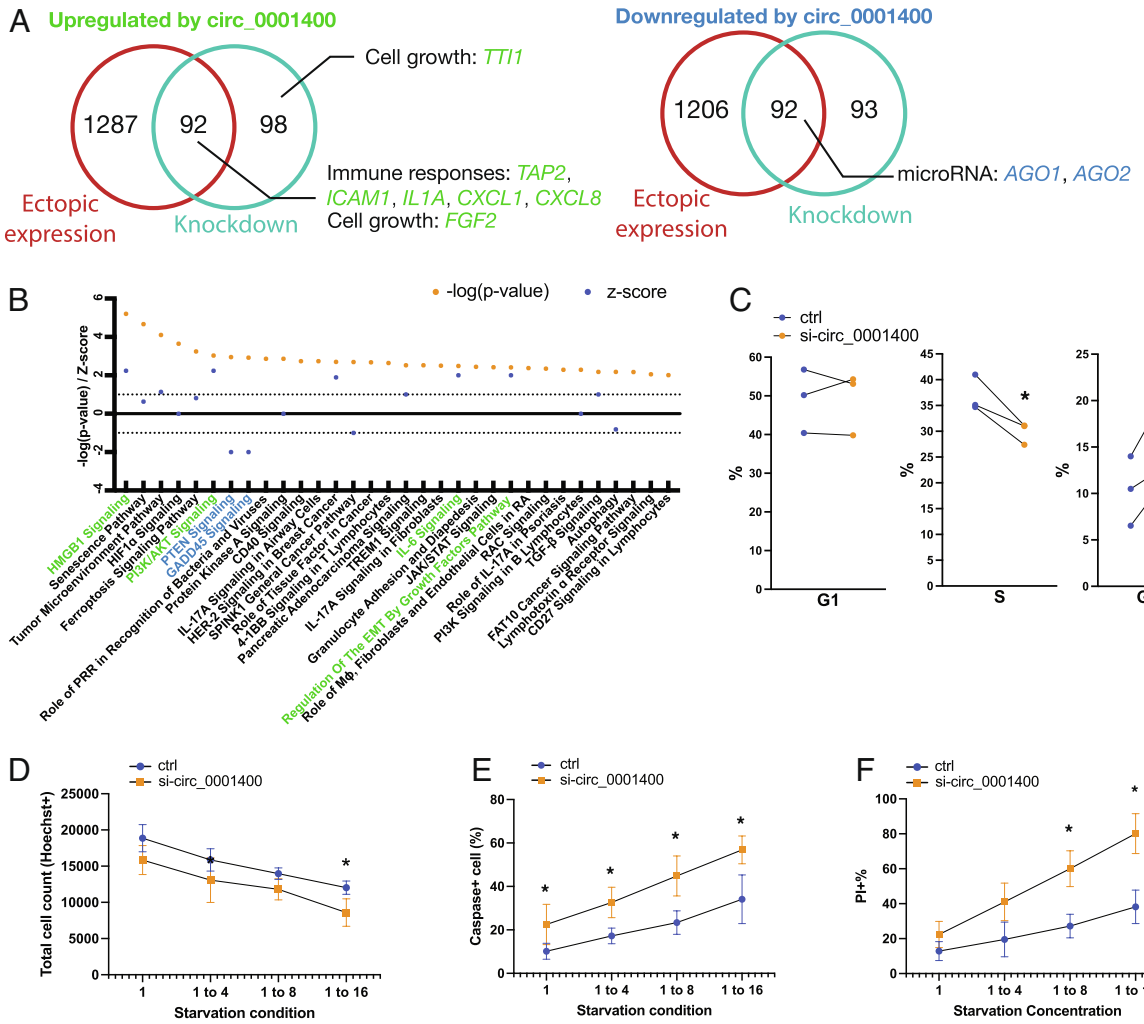

Fig. 5. circ_001400 promotes cell growth and induces immune reaction genes. (*A*) Venn diagrams are showing consistently differentially regulated genes (DEGs) by circ_0001400 in HUVECs. Cells were treated with siRNA targeted against circ_0001400 (n = 3) or infected with circ_0001400-expressing lentivirus (n = 3) followed by KSHV infection. DEGs are defined as having adjusted *P*-value <0.05 as calculated by voom (limma package). On 3 d post-infection, the total RNA was extracted for RNA-Seq. Select up-regulated (left Venn diagram) or down-regulated (right Venn diagram) genes by circ_0001400 are shown in green and blue, respectively. The list of DEGs is available in Dataset S4. (*B*) Pathway enrichment analysis of DEGs (*A*) by Ingenuity Pathway Analysis (Qiagen). Significance of pathway enrichment is shown as *P*-values. Z-scores describe the predicted activation or inhibition of pathways. Pathways are color-coded when |Z| > 1.96. (*C*) Cell cycle analysis of circ_0001400-depleted KSHV-infected cells. Infected cells were incubated with EdU at 3 d post-infection for 4 h, and cell cycles were quantitated by flow cytometry (n = 3). (*D*–*F*) Total, apoptotic, and dead cell quantitation of circ_0001400-depleted KSHV-infected cells. HUVECs were siRNA-treated for circRNA depletion and infected with KSHV for three days. The next day, the media was replaced with diluted media to the ratio as described. At 3 d post-infection, total cells were counted by Hoechst staining. Caspase3/7 substrates that emit signal upon cleavage were added to measure apoptosis rates. Dead cells were stained with propidium iodide. Cells were quantitated by high-content imaging (n = 3). Significances were calculated with paired-*t* tests. *P-value < 0.05.

by knockdown of the circRNA (Fig. 5 *E* and *F*), confirming the effects of this circRNA on pro-growth outcomes.

Simultaneously, activation of immunity-related pathways including high mobility group box 1 (HMGB1) signaling and IL-6 signaling, was correlated with circ_0001400 expression (Fig. 5*B*). Notably, DEGs include key genes involved in antigen presentation like *TAP2* (Transporter 2, ATP binding cassette subfamily B member) and *ICAM1* (Intercellular Adhesion Molecule 1) as well as various inflammatory cytokines and chemokines (Fig. 5*A*). ICAM1 is one of the co-stimulatory molecules, which are necessary to activate antiviral T cells. Depletion of circ_0001400 resulted in reduced transcript levels (Fig. 6*A*) as well as cell surface expression levels of co-stimulatory molecules for antigen presentation including ICAM1, as measured with flow cytometry (Fig. 6 *B* and *C*).

Circ_0001400 Interacts with an Mammalian Target of the Rapamycin (mTOR)-Component and Sustains Its Abundance. RNA–RNA interactions are one mechanism circRNAs use to alter gene regulation (8). We searched for RNAs associated with circ_0001400 using RNA-pulldown assays in 293T cells. A biotinylated DNA oligo that is complementary to the back-splice junction of circ_0001400 was used to pull down circ_0001400, and interacting RNAs were determined by deep-sequencing (Fig. 7*A*). To increase the sensitivity, cells were treated with psoralen followed by long-wave ultraviolet (UV) radiation, which covalently cross-links double-stranded RNAs. Extracted RNAs were exposed to short-wavelength UV to reverse the cross-linking. 15,234 transcripts were identified in all replicates, and 2,579 among them were found to be enriched by circRNA-specific probes (*SI Appendix*, Fig. S6 *A* and *B*). Primary component analysis showed the reproducibility and specificity of enriched transcripts (*SI Appendix*, Fig. S6*C*). The top candidate of interacting RNAs was shown in Dataset S5.

TTI1 and *CNOT10* mRNAs showed the highest enrichment as well as adjusted *P*-values (Fig. 7*B*). TTI1 is a component of mTOR complex and important in forming mTOR complexes (28–30),

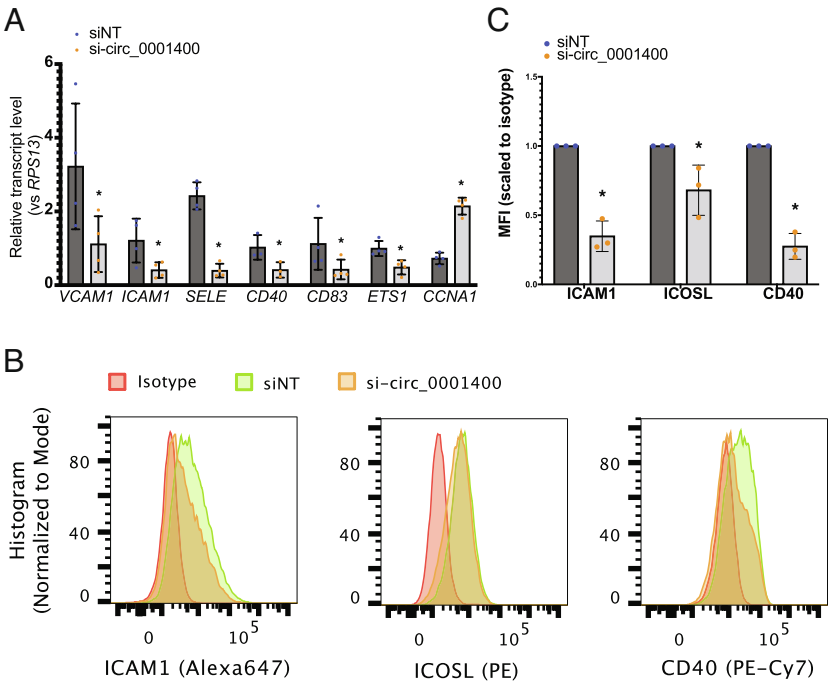

Fig. 6. circ_001400 activates immune gene expression and increases co-stimulatory molecules on cell surface. (*A*) Human transcript levels after circ_0001400 ectopic expression in KSHV-infected HUVECs (MOI 0.5 i.u.). Total RNAs were extracted 3 d post-infection for RT-qPCR (n = 3). Significances were calculated with paired-*t* tests. **P*-value < 0.05. (*B* and *C*) Immune staining of co-stimulatory molecules on circ_0001400-depleted KSHV-infected cells. At three dpi, cells were stained with antibodies specific to co-stimulators and isotypes (n = 3). Representative histograms are shown (*B*). Mean fluorescence intensity for each antibody was scaled to the signal from isotypes and shown in (*C*). Significances were calculated with paired-*t* tests. **P*-value < 0.05.

which is known to promote cell growth and inhibit lytic cycle of KSHV (30). CNOT10 is a component of the carbon catabolite repression 4–negative on TATA-less complex, which serves as a deadenylase and is critical for miRNA-mediated mRNA degradation (31). The interaction between circ_0001400 and these RNAs was confirmed with RT-qPCR (Fig. 7*C*). *PHPT1* and *SIVA1* showed only a mild enrichment (Dataset S5); RT-qPCR showed tendency of enrichment value but not statistically significant (Fig. 7*B*), indicating the use of both enrichment value and p-value is appropriate for finding interacting RNAs. RELL1, which overlaps with circ_0001400, and *ZKSCAN1*, part of which was used as a backbone of circ_001400 expression cassette, were also enriched indicating the successful pulldown of ectopically expressed circRNAs (Fig. 7*B*).

Since circ_0001400 activated PI3K/AKT signaling pathway and showed pro-growth, anti-lytic cycle phenotype, the regulation of *TTI1* mRNA levels by circ_0001400 was assessed. Depletion, but not ectopic expression, of circ_0001400 significantly alters the transcript level of *TTI1* in 293T cells (Fig. 7*D*). The same tendency was observed in primary endothelial cells (Fig. 5*A* and Dataset S4). Knockdown of *TTI1* in KSHV-infected LECs also showed the increase of replication and transcription activator (RTA) and LANA without affecting viral entry (Fig. 7*E* and *F*) as well as the tendency to increase virus production in all biological replicates (Fig. 7*G*). Interestingly, depletion of *PNISR*, another circ_0001400-interacting gene (Fig. 3), reduced KSHV gene expression, infection, and virus production (Fig. 3 *E*–*G*), whereas viral transcripts showed the tendency to increase as in *RELL1* (Fig. 3 *D* and *E*), suggesting PNISR's functions during infection in addition to splicing. These results allow a model that circ_0001400 interacts with *TTI1* to sustain its transcript levels (Fig. 8*A*). We thus identified RNAs that may account for pro-growth, inflammatory, and anti-lytic phenotypes caused by circ_0001400 in KSHV-infected cells.

Discussion

In KSHV-infected primary human endothelial cells, we found that circ_0001400 inhibited lytic gene expression and virus production, while the circRNA also promoted cell cycle and suppressed apoptosis. Though the former phenotypes apparently are antiviral and the latter pro-growth features are oncogenic and pro-viral, these phenotypes support the notion that circ_0001400 propagates infected cells that are in latency, during which only handful of viral genes (latent genes) are expressed and viruses are not produced (Fig. 8*B*). Switching to latent infection after infection is critical for herpesviruses like KSHV and EBV since this less immunogenic state allows viruses to evade immune surveillance and persist for the life of host. These wide ranges of phenotypes caused by circ_0001400 in primary endothelial cells are in stark contrast to our previous study in a renal carcinoma cell line, SLK (12). There, we observed the inhibition of viral gene expression, but, unlike primary endothelial cells as shown here (Figs. 5 and 6), cell growth or immune genes were not affected. circ_0001400 thus conferred only antiviral functions in SLK cells. This also signifies the importance to utilize models that are closer to clinical conditions, such as primary endothelial cells and *de novo* infection system.

We identified hsa_circ_0001400 to be induced by various human herpesviruses, KSHV, EBV, and HCMV. It is also noteworthy that the increase of the circRNAs occurs in wide range of cell types including epithelial cells, endothelial cells, fibroblasts, and B lymphocytes. Since circ_0001400 is just one of dozens of infection-induced circRNAs, these observations present the following question: Are there any other circRNAs also regulated in infection with various viruses and cell types? And, if so, what will be the aggregate effect of circRNAs in host-virus interactions? Circ_0001400 alone has already showed a significant role in cell growth and latency, and the potential of circRNAs, and ncRNAs as extension, should be highlighted.

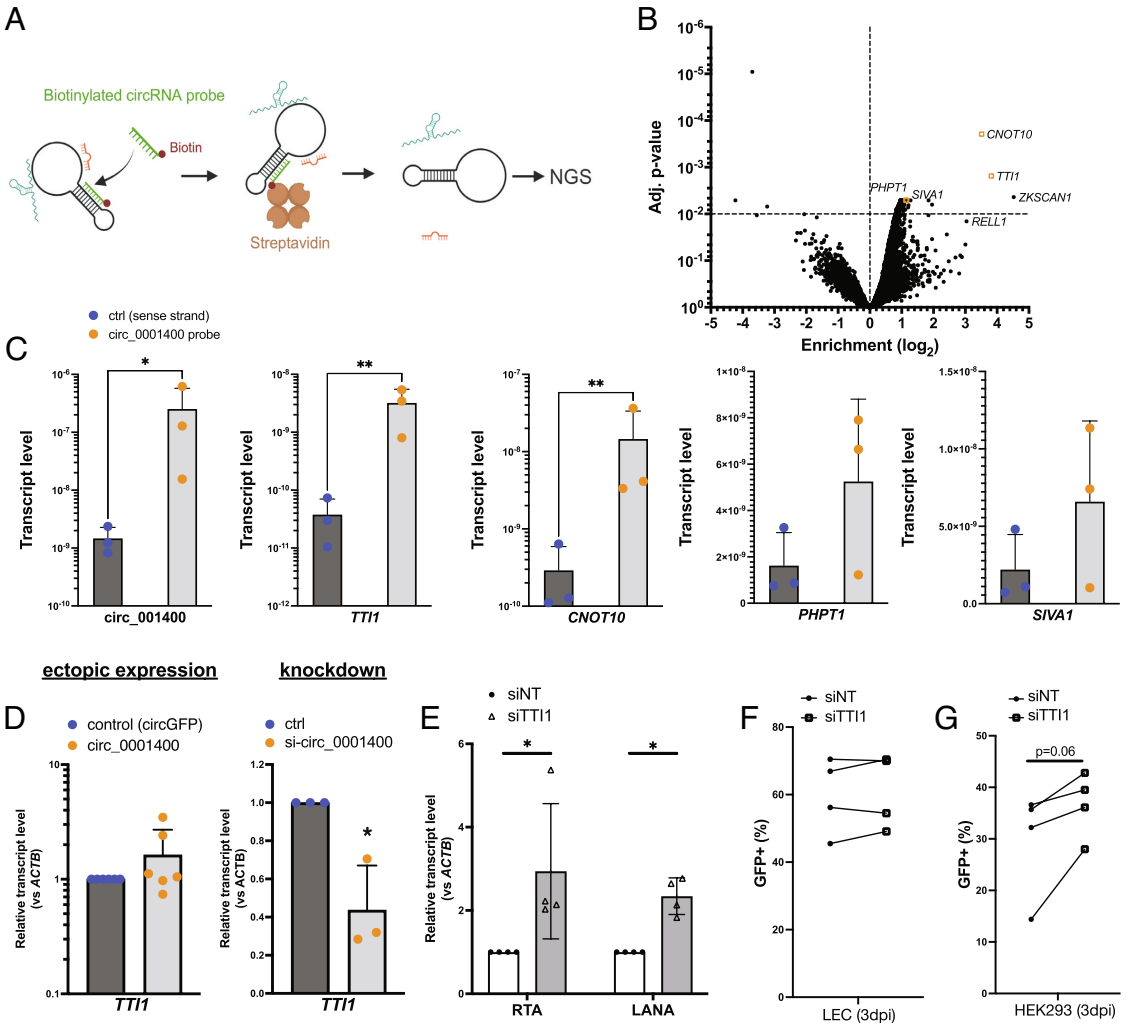

Fig. 7. circ_001400 interacts with mTOR-component *TTI1* and sustains its transcript level. (*A*) Diagram of the RNA-pulldown assay is shown. Total RNA was incubated with biotinylated DNA oligos that is specific to circ_0001400, and circRNA-RNA complexes are purified using streptavidin beads. Next-generation sequencing was performed to determine their identities. (*B*) A volcano plot of transcripts identified by the circ_0001400 RNA-pulldown assay in 293T cells. Mapped reads were median scaled, and enrichments were calculated by voom (limma package). *ZKSCAN1* and *RELL1* are partially included in the circ_0001400 expression plasmid vectors and thus serve as positive control of pulldown. Transcripts that were confirmed in Fig. 6*C* are depicted as orange rectangles. n = 3. (*C*) RT-qPCR of enriched transcripts after RNA-pulldown. circ_0001400 was ectopically expressed in 293T cells for 24 h, and RNA-pulldowns were performed (n = 3). Enrichment of circ_0001400 and candidate mRNAs (listed in Dataset S5) are shown. (*D*) *TTI1* transcript levels after manipulation of circ_0001400 transcript levels. circ_0001400 was ectopically expressed (n = 6) or depleted by siRNAs (n = 3) in 293T cells for 48 h. Total RNAs were extracted followed by RT-qPCR. (*E*) RNAi-mediated knockdown of TTI1. LECs were transfected with siRNAs targeting TTI1 followed by KSHV infection at MOI of 1.0 i.u. RNA was extracted 3 d post–infection, and transcript levels of viral transcripts were measured. N = 4. (*F*) Infection rates of *TTI1*-depleted LEC cells. LECs from (*E*) were quantified for GFP by flow cytometry. N = 4. (*G*) Virion production of *TTI1*-depleted LEC cells. Conditioned media was collected from LECs from (*F*), and HEK-293 cells were incubated with the conditioned media for 3 d. Infected HEK-293 cells were counted by GFP signals with flow cytometry. N = 4 and significances were calculated with paired-*t* tests. **P*-value < 0.05.

Stimulating the PI3K/AKT/mTOR pathway is critical for KSHV infection. The pathway is simulated by multiple viral proteins, like K1, viral G protein-coupled receptor (vGPCR) (ORF74), vIL-6 (K2), and ORF45. KSHV induces the PI3K pathway upon de novo infection to promote cell growth and reduce apoptosis (32) as well as maintaining latency (33). mTOR is also known to induce immune genes like ICAM1 via NF-kB pathway in HUVECs (34). Consistently, we observed same pro-growth phenotypes, activation of immune genes, and inhibition of lytic cycles by circ_0001400. RNA-pulldown assay showed the circRNA's interaction with a mTOR component, *TTI1*, and circ_0001400 sustains transcript levels of *TTI1* in 293T cell and HUVECs. Further, *TTI1* is one of PEL-specific oncogenic dependencies (35) indicating its importance in KSHV-driven oncogenesis. Knockdown of *TTI1* in endothelial cells at least partially phenocopied circ_0001400. It is therefore likely that circ_0001400 causes pro-latency phenotypes via maintaining PI3K/AKT/mTOR pathway. These phenotypes are, in general, moderate even with strong ectopic expression with lentivirus (Figs. 4–6 and *SI Appendix*, Fig. S1*B*), suggesting circ_0001400's fine-tuning capability. It should be, however, noted that it is one of many human and viral circRNAs that are induced upon infection and, in aggregate, circRNAs may have more robust functions.

Immune regulatory effects of circ_0001400 were suggested by transcriptomic data. Co-stimulators of antigen presentations such as ICAM1 are well documented to be suppressed by KSHV (36). On the other hand, induction of circ_0001400 upon KSHV infection increased co-stimulators including ICAM1, which may lead to higher immunogenicity and removal of infected cells by host immune surveillance system. Recently, another circRNA from the same gene, circ_0002194 (consist of exon5-6 of *RELL1*, as opposed to exon4-6 of circ_0001400), was also found to induce ICAM1 and VCAM1 in HUVECs (37). circ_0002194 was proposed to sponge miR-6873-3p, which resulted in increase of MyD88 as well as its

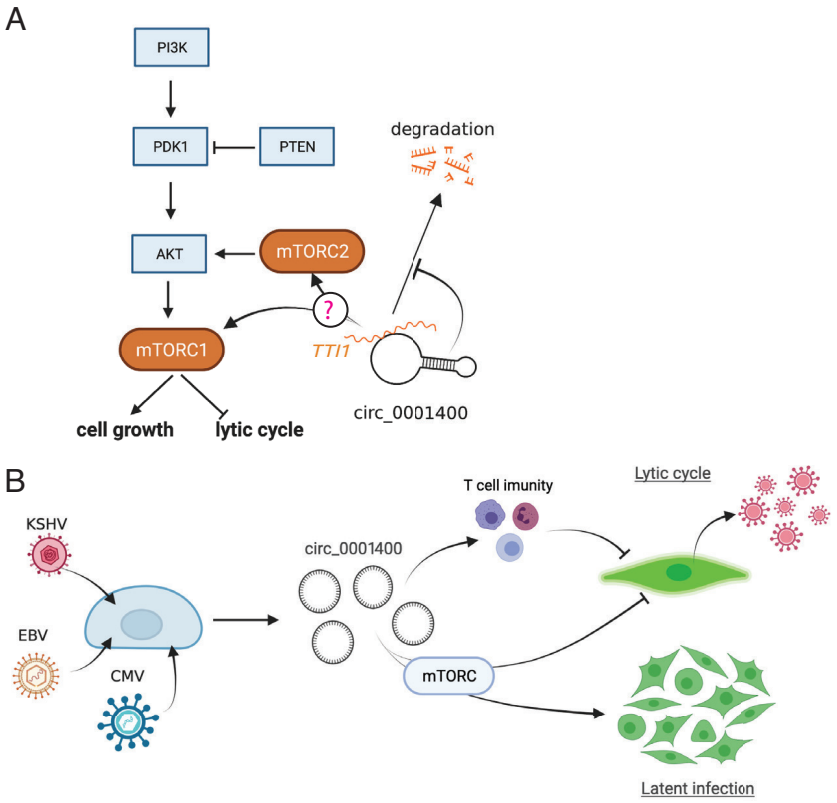

Fig. 8. Model of hsa_circ_0001400 in virus-host interactions. (*A*) Proposed model of circ_0001400's regulation of PI3K/AKT/mTOR pathway. (*B*) hsa_circ_0001400 is induced by multiple herpesviruses. The circRNA allows activation of PI3K/AKT/mTOR pathway and promotes cell growth of latently KSHV-infected cells. On the other hand, lytic infection is suppressed by inhibition of virus production and increase of co-stimulatory molecules by circ_0001400.

downstream genes, *ICAM1* and *VCAM1*. Though circ_0002194 was not detectable and Myd88 was not identified to be regulated by circ_0001400 in our datasets (Dataset S4), it is still possible that miR-6873-3p is responsible for the induction of cell surface markers. In addition, genes coding for inflammatory cytokines and chemokines, *IL1A*, *CXCL1*, *CXCL8* (coding for IL-8), are also induced by circ_0001400. This may suggest fine-tuning of immunogenicity by host circRNAs. Though immune evasion by reducing antigen presentation is important and necessary, removal of excessively immunogenic cells, i.e., lytic cells, potentially via circ_0001400, is beneficial to maintain latent infection in vivo by avoiding antiviral inflammatory microenvironment at infection sites (Fig. 8).

RNA-binding proteins were recently found to interact with certain circRNAs (38). Our CARPID dataset therefore can be utilized to search for such proteins interacting with circ_0001400 in future studies. Among enriched circRNA-interacting proteins, one apparent omission was the Argonaut family of proteins, core proteins of RNA-induced silencing complex (RISC). This was unexpected since some circRNA regulatory mechanisms include acting as decoys or "sponges" for miRNAs. It is possible that because circ_0001400 is relatively short at 434 nucleotides, there are no enriched binding sites of particular miRNAs. Well-studied miRNA sponge circRNA CDR1as is 1.5 kb and harbors ~70 miR-7 binding sites. In silico prediction did not find such concentrated miRNA-binding sites of circ_0001400. Since circ_0001400 was suggested to control *AGO1*, *AGO2*, and *CNOT10*, this circRNAs may regulate general miRNAs machinery, rather than targeting specific miRNAs.

Another surprising observation on the circ_0001400's interactions is, at least for *TTI1*, depletion of circ_0001400 reduced the amount of the interacting RNAs (8). Though circRNAs are conventionally known to suppress bound RNAs, there is an example that circRNAs maintain levels of a bound miRNA (39). It is unclear whether circ_0001400 binds to mRNAs directly or indirectly yet, but similar circRNA-mediated RNA maintenance may play a role for the circ_0001400's gene regulatory mechanism.

We also explored the mechanism by which KSHV infection increased the amounts of circRNAs. Here, we show that most of differentially regulated circRNAs by infection are regulated at co-transcriptional levels, including circ_0001400, likely at back-splicing steps. We have previously shown that circ_0001400 synthesis depends on multiple RBPs like fused in sarcoma (FUS) and quaking (QKI) (12). We newly identified PNISR to interact with circ_0001400. Since PNISR is reported to be a splicing factor (40), it is another candidate to be involved in the synthesis of circ_0001400. Indeed, knockdown of PNISR resulted in biased production of mRNAs compared to circRNAs from *RELL1* locus and showed the tendency to increase viral linear transcripts. Interestingly, contrary to the effect on viral gene expression, PNISR depletion reduced KSHV infection. This may suggest KSHV's dependence of in splicing controls by PNISR, but further research is warranted to prove this hypothesis.

How different herpesviruses regulate same circRNAs is still an open question. If PNISR and other candidates are specific to circ_0001400 unlike FUS/QKI, which are known to regulate wide range of circRNAs (8), these proteins may be critical to reveal how KSHV induces specific circRNAs; the specificity of those RBPs that regulates the ratio of forward- vs back-splicing determines which circRNAs are to be induced or decreased upon infection. Functional analysis of these splice factors may lead to deeper understanding of viral regulation of circRNAs, which can potentially be clinical targets. In addition, tipping the balance of splicing to back-splicing may be not enough for different herpesviruses to induce circRNAs; some universal mechanism such as interferon responses may be involved in the circRNA induction. *RELL1*, for

example, was reported to be induced in all subtypes of IFN-α (41). In addition, oxidized low-density lipoprotein (ox-LDL) was found to induce circ_0002194 (family of circ_0001400) (37). Since infection with herpesviruses induces reactive oxygen species (42), which forms ox-LDL, the oxidative stress may be also responsible for the induction of specific circRNAs.

In conclusion, we identified the circRNA that is induced by KSHV infection and promotes the growth of latently infected cells while suppressing lytic cycle early after infection. Since maintaining latent infection is crucial for oncogenic viruses, hsa_circ_0001400 may have wider implications in other viruses. Circ_0001400 is one of many host circRNAs induced upon infection, and the investigation of more circRNAs will uncover this new layer of virus-host interactions via ncRNAs.

Materials and Methods

Cell Culture. HUVECs and Human Dermal LEC were obtained from Lonza and PromoCell, respectively, and passaged in EGM2 medium (Lonza) for up to five passages, with passages three to five used for experiments. Media was replaced every 2 d. HEK-293 and 293T cells (American Type Culture Collection (ATCC)) were maintained in Dulbecco's modified Eagle medium (DMEM) supplemented with 10% Fetal Bovine Serum (FBS) (Gibco), penicillin (100 U/mL; Gibco), and streptomycin (100 mg/mL; Gibco). Vero (ATCC) was maintained in DMEM (Gibco) supplemented with 5% FBS, 1 mM sodium pyruvate, 2 mM L-glutamine, and 100 U/mL penicillin-streptomycin. MRC5 (ATCC) was maintained in DMEM supplemented with 10% FBS, 1 mM sodium pyruvate, 2 mM L-glutamine, and 100 U/mL penicillin-streptomycin. The infected iSLK cell line (WT BAC16 strain) is a gift from Rolf Renne (1). They were maintained in DMEM supplemented with 10% FBS, penicillin, streptomycin, hygromycin (1,200 μg/mL), puromycin (1 μg/mL), and G418 (250 μg/mL). EBV-positive and negative Akata cell lines were maintained in Roswell Park memorial institute (RPMI) medium supplemented with 10% FBS, penicillin, and streptomycin. Cells were cultivated at 37 °C in a 5% CO_2 incubator.

Virus Production (iSLK) and Infection. For KSHV, BAC16 virus stock was prepared by inducing lytic cycle in iSLK-BAC16 cells with doxycycline (1 μg/mL; Sigma-Aldrich) and sodium butyrate (1 mM; Cayman Chemical) for 3 d. Collected supernatants were cleared of debris with centrifugation at 500 × g for 5 min, filtered (Rapid-Flow 0.45 μm filter; Nalgene), and pelleted with centrifugation at 30,000 g for 16 h. The virus pellet was resuspended to EBM2 (Lonza) media. Titration method was adapted from a previous report (43). HUVECs or LECs were infected for 3 d, and the GFP-positive population was quantified by CytoFLEX S (Beckman Coulter). Here, one infectious unit (i.u.) of multiplicity of infection (MOI) was defined as the amount of viruses enough to infect all LECs if virions are distributed equally in the culture. For HSV-1, Vero cells were infected at a low MOI (~0.01 plaque forming units (PFU)/cell) with strain KOS and harvested when cells were sloughing from the sides of the vessel. Supernatant and cell fraction were collected and centrifuged at 4,000 × g 4 °C for 10 min. The subsequent supernatant fraction was reserved. The pellet fraction was freeze (−80 °C 20 min)/thawed (37 °C 5 min) for three cycles, sonicated for 1 min, and centrifuged at 2,000 × g 4 °C for 10 min. The final virus stock was composed of the cell-associated virus and reserved supernatant virus fractions. Virus titers were assessed by plaque assay in Vero cells.

De novo infections of KSHV in HUVECs and LECs were carried out by diluting concentrated supernatant in EGM2 medium at a MOI of 1.0 i.u. unless otherwise mentioned. Polybrene (Millipore) was added at 8 μg/mL. Virus supernatant was washed off after overnight incubation and replaced with fresh EGM2. Cells were refed every 2 d until harvest. For HSV-1, confluent MRC5 cells were infected with ten PFU strain KOS per cell. Virus was adsorbed in PBS for 1 h at room temperature. Viral inoculum was removed, and cells were washed quickly with PBS before adding on DMEM media supplemented with 2% FBS. 0 h time point was considered after adsorption of infected monolayers when cells were place at 37 °C to incubate.

Data Analysis. Most graphs contain plots with each data point represented and include the mean and SDs. For testing of significance, paired-*t* tests were performed with Prism (GraphPad) except for high-throughput analysis like RNA-Seq and microarray and presented with asterisks indicating *P*-values.

Data, Materials, and Software Availability. Sequencing and microarray data produced in this work are available at Gene Expression Omnibus (GSE206930) (15) and Sequence Read Archive (PRJNA851845, PRJNA851702, and PRJNA851589) (17, 20, 21).

ACKNOWLEDGMENTS. This work was supported by the Intramural Research Program of the Center for Cancer Research, National Cancer Institute, NIH (1ZIABC011176), and Japan Society for the Promotion of Science (Research Fellowship for Japanese Biomedical and Behavioral Researchers at NIH). The funders had no role in study design, data collection and analysis, decision to publish, or preparation of the manuscript. We thank the Center for Cancer Research Sequencing Facility (Frederick, MD) for their assistance in sequencing libraries. We thank Yuichi Abe, Aichi Cancer Center Research Institute, for a valuable discussion about proteomics data analysis. The resources of the NIH High-Performance Computing BIOWULF Cluster were utilized for all our computational needs. Figures are partially created with BioRender.com.

Author affiliations: [a]HIV and AIDS Malignancy Branch, Center of Cancer Research, National Cancer Institute, Bethesda, MD 20892; [b]Center for Cancer Research Collaborative Bioinformatics Resource, Center for Cancer Research, National Cancer Institute, NIH, Bethesda, MD 20892; [c]Advanced Biomedical Computational Sciences, Frederick National Laboratory for Cancer Research, Leidos Biomedical Research, Inc., Frederick, MD 21701; and [d]Protein Characterization Laboratory, Cancer Research Technology Program, Frederick National Laboratory for Cancer Research, Leidos Biomedical Research, Inc., Frederick, MD 21701

1. M. K. White, J. S. Pagano, K. Khalili, Viruses and human cancers: A long road of discovery of molecular paradigms. *Clin. Microbiol. Rev.* **27**, 463–481 (2014).
2. C. Shannon-Lowe, A. Rickinson, The global landscape of EBV-associated tumors. *Front. Oncol.* **9**, 713 (2019).
3. P. Sarnow, S. M. Sagan, Unraveling the mysterious interactions between Hepatitis C virus RNA and liver-specific MicroRNA-122. *Ann. Rev. Virol.* **3**, 1–24 (2015).
4. C. C. Rossetto, G. S. Pari, PAN's Labyrinth: Molecular biology of Kaposi's sarcoma-associated herpesvirus (KSHV) PAN RNA, a multifunctional long noncoding RNA. *Viruses* **6**, 4212–4226 (2014).
5. Q. Yin *et al.*, MicroRNA-155 is an Epstein-Barr virus-induced gene that modulates Epstein-Barr virus-regulated gene expression pathways. *J. Virol.* **82**, 5295–5306 (2008).
6. R. L. Skalsky *et al.*, Kaposi's sarcoma-associated herpesvirus encodes an ortholog of miR-155. *J. Virol.* **81**, 12836–12845 (2007).
7. F. Lu *et al.*, Epstein-Barr virus-induced miR-155 attenuates NF-kappaB signaling and stabilizes latent virus persistence. *J. Virol.* **82**, 10436–10443 (2008).
8. L. S. Kristensen *et al.*, The biogenesis, biology and characterization of circular RNAs. *Nat. Rev. Genet.* **20**, 675–691 (2019).
9. S. Memczak *et al.*, Circular RNAs are a large class of animal RNAs with regulatory potency. *Nature* **495**, 333–338 (2013).
10. T. B. Hansen *et al.*, Natural RNA circles function as efficient microRNA sponges. *Nature* **495**, 384–388 (2013).
11. T. Tagawa *et al.*, Discovery of Kaposi's sarcoma herpesvirus-encoded circular RNAs and a human antiviral circular RNA. *Proc. Natl. Acad. Sci. U.S.A.* **115**, 201816183 (2018).
12. T. Tagawa *et al.*, Characterizing expression and regulation of gamma-herpesviral circular RNAs. *Front. Microbiol.* **12**, 670542 (2021).
13. T. Toptan *et al.*, Circular DNA tumor viruses make circular RNAs. *Proc. Natl. Acad. Sci. U.S.A.* **115**, E8737–E8745 (2018).
14. N. A. Ungerleider *et al.*, Comparative analysis of gammaherpesvirus circular RNA repertoires: Conserved and unique viral circular RNAs. *J. Virol.* **93**, e01952-18 (2019).
15. J. Ziegelbauer, Kaposi's sarcoma herpesvirus induces host circular RNAs and maintain latent infection. *Gene Expression Omnibus*. https://0-www-ncbi-nlm-nih-gov.brum.beds.ac.uk/geo/query/acc.cgi?acc=GSE206930. Deposited 25 June 2022.
16. A. Oberstein, T. Shenk, Cellular responses to human cytomegalovirus infection: Induction of a mesenchymal-to-epithelial transition (MET) phenotype. *Proc. Natl. Acad. Sci. U.S.A.* **114**, E8244–E8253 (2017).
17. S. Dremel, Total RNA-Seq in HSV-1 infected human fibroblasts. *Sequence Read Archive*. https://www.ncbi.nlm.nih.gov/bioproject/PRJNA851702/. Deposited 27 July 2022.
18. X.-K. Ma *et al.*, CIRCexplorer3: A CLEAR pipeline for direct comparison of circular and linear RNA expression. *Genom. Proteom. Bioinform.* **17**, 511–521 (2019).
19. A. K. P. Serquiña, T. Tagawa, D. Oh, G. Mahesh, J. M. Ziegelbauer, 25-hydroxycholesterol inhibits Kaposi's sarcoma herpesvirus and Epstein-Barr virus infections and activates inflammatory cytokine responses. *mBio* **12**, e0290721 (2021).
20. S. Dremel, 4SU-Seq of KSHV lytic reactivation in iSLK-BAC16 model. *Sequence Read Archive*. https://www.ncbi.nlm.nih.gov/bioproject/PRJNA851589/. Deposited 8 August 2022.
21. S. Dremel, Total RNA-Seq in KSHV Infection Models. Sequence Read Archive. https://www.ncbi.nlm.nih.gov/bioproject/PRJNA851845/. Deposited 8 August 2022.

22. W. Yi *et al.*, CRISPR-assisted detection of RNA–protein interactions in living cells. *Nat. Methods* **17**, 685–688 (2020).
23. S. Li *et al.*, Screening for functional circular RNAs using the CRISPR–Cas13 system. *Nat. Methods* **18**, 51–59 (2021).
24. D. Liang, J. E. Wilusz, Short intronic repeat sequences facilitate circular RNA production. *Genes Dev.* **28**, 2233–2247 (2014).
25. C. Arias *et al.*, KSHV 2.0: A comprehensive annotation of the Kaposi's sarcoma-associated herpesvirus genome using next-generation sequencing reveals novel genomic and functional features. *PLoS pathog.* **10**, e1003847 (2014).
26. F. Cheng *et al.*, KSHV-initiated notch activation leads to membrane-type-1 matrix metalloproteinase-dependent lymphatic endothelial-to-mesenchymal transition. *Cell Host Microbe* **10**, 577–590 (2011).
27. M. J. Eramo, C. A. Mitchell, Regulation of PtdIns(3,4,5)P3/Akt signalling by inositol polyphosphate 5-phosphatases. *Biochem. Soc. Trans.* **44**, 240–52 (2016).
28. H. Takai, Y. Xie, T. de Lange, N. P. Pavletich, Tel2 structure and function in the Hsp90-dependent maturation of mTOR and ATR complexes. *Genes Dev.* **24**, 2019–2030 (2010).
29. T. Kaizuka *et al.*, Tti1 and Tel2 are critical factors in mammalian target of rapamycin complex assembly. *J. Biol. Chem.* **285**, 20109–16 (2010).
30. M. Pal *et al.*, Structure of the TELO2-TTI1-TTI2 complex and its function in TOR recruitment to the R2TP chaperone. *Cell Rep.* **36**, 109317 (2021).
31. Y.-T. Shirai, T. Suzuki, M. Morita, A. Takahashi, T. Yamamoto, Multifunctional roles of the mammalian CCR4–NOT complex in physiological phenomena. *Front. Genet.* **5**, 286 (2014).
32. A. P. Bhatt, B. Damania, AKTivation of PI3K/AKT/mTOR signaling pathway by KSHV. *Front. Immunol.* **3**, 401 (2013).
33. L. Peng *et al.*, Inhibition of the phosphatidylinositol 3-kinase-Akt pathway enhances gamma-2 herpesvirus lytic replication and facilitates reactivation from latency. *J. Gen. Virol.* **91**, 463–469 (2010).
34. M. Minhajuddin, F. Fazal, K. M. Bijli, M. R. Amin, A. Rahman, Inhibition of mammalian target of rapamycin potentiates thrombin-induced intercellular adhesion molecule-1 expression by accelerating and stabilizing NF-kappa B activation in endothelial cells. *J. Immunol.* **174**, 5823–5829 (2005).
35. M. Manzano *et al.*, Gene essentiality landscape and druggable oncogenic dependencies in herpesviral primary effusion lymphoma. *Nat. Commun.* **9**, 3263 (2018).
36. H.-R. Lee, K. Brulois, L. Wong, J. U. Jung, Modulation of immune system by Kaposi's Sarcoma-associated herpesvirus: Lessons from viral evasion strategies. *Front. Microbiol.* **3**, 44 (2012).
37. H. Huang, X. Huang, H. Yu, Y. Xue, P. Zhu, Circular RNA circ-RELL1 regulates inflammatory response by miR-6873-3p/MyD88/NF-κB axis in endothelial cells. *Biochem. Biophys. Res. Commun.* **525**, 512–519 (2020).
38. A. Huang, H. Zheng, Z. Wu, M. Chen, Y. Huang, Circular RNA-protein interactions: Functions, mechanisms, and identification. *Theranostics* **10**, 3503–3517 (2020).
39. M. Piwecka *et al.*, Loss of a mammalian circular RNA locus causes miRNA deregulation and affects brain function. *Science* **8**, eaam8526 (2017).
40. G. Zimowska *et al.*, Pinin/DRS/memA Interacts with SRp75, SRm300 and SRrp130 in Corneal Epithelial Cells. *Invest. Opthalmol. Vis. Sci.* **44**, 4715 (2003).
41. J. Schuhenn *et al.*, Differential interferon-α subtype induced immune signatures are associated with suppression of SARS-CoV-2 infection. *Proc. Natl. Acad. Sci. U.S.A.* **119**, e2111600119 (2022).
42. L. Tao *et al.*, Reactive oxygen species oxidize STING and suppress interferon production. *Elife* **9**, e57837 (2020).
43. T. Tagawa *et al.*, Epstein-Barr viral miRNAs inhibit antiviral CD4+ T cell responses targeting IL-12 and peptide processing. *J. Exp. Med.* **213**, 2065–2080 (2016).